INT. J. REMOTE SENSING, 1981, VOL. 2, NO. 1, 71–82

Remote sensing of bottom reflectance and water attenuation parameters in shallow water using aircraft and Landsat data

DAVID R. LYZENGA

Environmental Research Institute of Michigan, Ann Arbor, Michigan 48107, U.S.A.

(Received 19 August 1980; revision received 19 November 1980)

Abstract. The reflectance of shallow water areas to solar illumination is a function of the water depth, the water optical properties and the bottom reflectance. Assuming the water optical properties to be uniform over a given scene area, the signals recorded by a multispectral scanner system may be combined to obtain information on the water attenuation and bottom reflectance parameters without knowledge of the water depth. These techniques are described and evaluated for a test site near North Cat Cay in the Bahamas.

1. Introduction

Conventional remote sensing techniques deal with the extraction of geological and biological information from land surface reflectance patterns as recorded by photographic or multispectral scanner (MSS) systems. The same kinds of inferences can be made from bottom reflectance patterns in shallow water. However, the bottom reflectance is not directly observable since it is modified by the effects of absorption and scattering in the overlying water column. In principle, these effects could be calculated if the water depth and water optical properties were known at each point in the scene. Frequently, the water optical properties may be considered uniform over fairly large areas because of horizontal mixing, but the water depth is highly variable and is generally not known throughout the scene. For this reason a technique was proposed (Lyzenga 1978) for combining the information in various spectral bands to produce a depth-invariant index of the bottom type. The input parameters required for this algorithm are the ratios of the water attenuation coefficients for the wavelength bands used. In this paper a method for obtaining these parameters from the MSS data is described, an example of the application of the bottom-recognition algorithm to aircraft and Landsat MSS data is presented, and the results of this application are evaluated using field measurements and aerial photography over North Cat Cay in the Bahamas.

2. Data collection

The test site selected for this evaluation is located on the western edge of the Great Bahama Bank, about 90 km east of Miami, Florida, and 15 km south of Bimini. The bottom in this area is composed largely of white carbonate sand with some rock and coral formations, and heavy growths of vegetation (mainly *Thalassia*) in protected areas. The water is very clear, approximating Jerlov's oceanic type II (Jerlov 1976), and extensive shallow areas exist with depths ranging from 1 to 15 m, dropping off to very great depths at the edge of the Bank.

Measurements of the irradiance attenuation coefficient of the water were made at

0143-1161/81/0201 0071 $02.00

several locations in the Great Bahama Bank in October 1977, using a Kahl subm photometer with filters approximating the Landsat green (MSS4, 0·5–0·6 μm) an (MSS5, 0·6–0·7 μm) bands. Two of these measurements were taken near the N Cat Cay test site, on 4 and 5 October 1977. Reduction of this data is describ §6. Landsat data was also collected over the test site on 11 October 1977. The La MSS data was collected in high gain mode and exhibits a large amount of stri which was corrected prior to the processing described in this paper.

The test site was revisited in August 1978, at which time a set of observations c bottom type and water depth were made at nine stations around North Cat Underwater photographs were taken and were subsequently analysed, as desc in §6, in order to extract the bottom reflectance at each station. Aircraft MSS dat also collected at this time using the ERIM M-8 multispectral scanner system (H *et al.* 1977). This data was collected at an altitude of 3·3 km, with a spatial resol of approximately 8 m, as compared to the Landsat spatial resolution of 79 m. spectral resolution of the aircraft scanner was also somewhat higher than the Lar MSS, with bandwidths of the order of 0·05 μm for the wavelength bands used. aircraft data included some sun glint and path radiance effects, which were rem during a preprocessing step.

3. Algorithm description

The technique previously described (Lyzenga 1978) for extracting bottom-information from MSS data depends upon the fact that the bottom-reflected radi is approximately a linear function of the bottom reflectance and an expone function of the water depth. Thus, when the measured radiances are transfor according to the following equation

$$X_i = \ln (L_i - L_{si})$$

where L_i is the measured radiance in band i and L_{si} is the deep-water radiance. resulting variables are linear functions of the water depth and are linearly relate each other, for a given bottom reflectance. That is, if X_i is plotted versus X_j and water depth is varied, the data points will fall along a straight line whose slop K_i/K_j, where K_i is the irradiance attenuation coefficient of the water in band i. I bottom reflectance is changed, the data points will fall along a parallel line whic displaced from the first. Thus, by measuring the amount of this displacement, a cha in the bottom reflectance can be detected even if the water depth is not known. amount of this displacement is given by

$$Y_i = \frac{K_j \ln (L_i - L_{si}) - K_i \ln (L_j - L_{sj})}{\sqrt{(K_i^2 + K_j^2)}}$$

by simple geometric reasoning. Under the assumption that the bottom-refle radiance $(L_i - L_{si})$ is proportional to the bottom reflectance and exponenti dependent on the water depth, the variable Y_i is independent of the water depth an related to the bottom reflectance as follows:

$$Y_i = Y_{i0} + \frac{K_j \ln r_i - K_i \ln r_j}{\sqrt{(K_i^2 + K_j^2)}}$$

where r_i is the bottom reflectance in band i and Y_{i0} is a constant for fixed illuminat and atmospheric conditions.

This procedure can be implemented as an MSS data processing algorithm

calculating the variable Y_i at each point in the scene, and using this variable as a depth-invariant index of the bottom type. If only two wavelength bands are involved, this variable would represent the end-point of the processing and could be used, for example, to generate a film image on which the density is proportional to the Y_i value. This image could then be interpreted as a map of the bottom reflectance, in which the effects of water depth variations have been removed. Alternatively, this index could be calculated for a number of band pairs and the resulting set of Y_i values could be used as inputs to a multispectral pattern recognition or classification routine in order to categorize the bottom into a set of discrete classes. In that case, the algorithm could be viewed as a preprocessing step to remove the effects of water depth variations, analogous to existing routines for removing atmospheric effects or scan angle variations.

In any case, the parameters required for operating this algorithm are the water attenuation coefficients, or actually only the ratios of the water attenuation coefficients in the wavelength bands used. These could conceivably be obtained by *in situ* measurements, but obviously it would be desirable to extract the required parameters from an analysis of the MSS data itself. A supervised procedure for obtaining the attenuation parameters, which requires some judgement and therefore cannot yet be completely automated, is described below.

A procedure for obtaining water attenuation parameters from shallow-water MSS data is suggested by the linear dependence of the X_i variables on the water depth. If a set of radiance measurements is made over an area of variable depth but uniform bottom reflectance, a linear correlation would be expected between any two of the variables X_i and X_j. An analysis of this correlation would then yield the ratio of the attenuation coefficients in the two wavelength bands used. This procedure does not yield the correct results, however, if the bottom reflectance varies with depth within the area selected. Thus, the problem is to select an area of uniform bottom reflectance for the analysis. This selection process is directly analogous to the process of training set selection in conventional supervised classification techniques used in remote sensing. The selection may be done on the basis of field observations and/or photographic interpretation using colour aerial photography. Alternatively, an analysis of

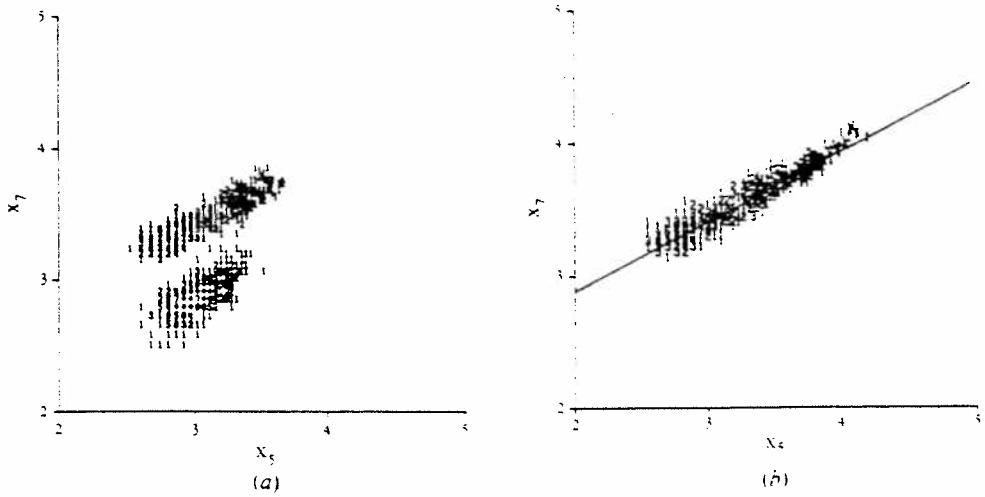

Figure 1. Scatter plot of X-values for aircraft bands C5 and C7: (*a*) mixed bottom (sand and vegetation); (*b*) sand bottom (line indicates least-squares fit to data).

the self-consistency of the data can be done to determine the uniformity of the trainir set. In this case, a uniform bottom is indicated by a high correlation among the variables, and this condition can usually be identified by an inspection of scatter plo of the data. Figure 1 (*a*) shows a scatter plot of X_i values over an area containing mixture of bottom types, while figure 1 (*b*) shows the distribution of the same variab over a uniform sand bottom.

Having selected a training set, a conventional least-squares regression analys may be done to determine the ratio of attenuation coefficients. The disadvantage this procedure, however, is that the results depend upon which variable is chosen be the dependent variable, since the mean square deviation from the regression line calculated in the direction of this variable. A better procedure is to determine the li for which the mean square deviation measured perpendicular to the line is minimize This procedure results in the equation

$$K_i/K_j = a - \sqrt{(a^2 - 1)}$$

where

$$a = \frac{\sigma_{ii} - \sigma_{jj}}{2\sigma_{ij}}$$

and

$$\sigma_{ij} = X_i X_j - X_i X_j$$

(i.e. σ_{ii} is the variance of the X_i measurements, σ_{jj} is the variance of the X_j measur ments, and σ_{ij} is the covariance of X_i and X_j). This equation yields a result which do not depend on the order in which the variables are selected.

4. Aircraft data analysis

The aircraft MSS records a digital signal which is proportional to the radiance each point in the scene. The radiance within each of the spectral bands indicated table 1 is recorded separately, and with a different proportionality constant dependi on the gain settings selected by the operator. The proportionality constants relat the digital signals to the radiances in each band could be determined by an analy of the calibration data recorded by the MSS, but since the bottom recognition algorit does not require absolute radiances this calibration was not attempted.

The first step in the analysis procedure is to determine the deep-water signals. T is accomplished by averaging the signals over a portion of the scene within which contribution due to bottom reflectance is negligible. For the scene under considerat

Table 1. Spectral bands recorded by the M-8 scanner system.

Band designation	Wavelength (μm)
C9	0·48–0·52
C8	0·50–0·54
C7	0·52–0·57
C6	0·55–0·60
C5	0·58–0·64
C4	0·62–0·70
C2	0·67–0·94
A1	Thermal IR

such an area was easily located off the edge of the Bank where the water depths are of the order of several hundred metres. Having determined the deep-water signals the X_i variables were computed and scatter plots similar to those shown in figure 1 were generated for each band pair. Scatter plots were generated for several areas in an attempt to locate an area of homogeneous bottom, as indicated by the linear distribution shown in figure 1 (*b*), which was obtained from an area just west of North Cat Cay. Ratios of the water attenuation coefficients were then calculated as outlined in the preceding section. The results are shown in table 2. Unfortunately, no *in situ* water optical measurements were made at the time of the overflight, but the ratios shown in table 2 are within the range expected for oceanic water.

Table 2. Ratios of water attenuation coefficients determined from aircraft MSS data.

Band pair	Ratio of attenuation coefficients
C9/C4	0·28
C8/C4	0·29
C7/C4	0·33
C6/C4	0·37
C5/C4	0·64

The choice of wavelength bands to be used in the bottom-recognition processing is determined by a trade-off between depth of penetration and sensitivity to reflectance changes. For a small change (Δr) in the bottom reflectance (r), assuming the fractional change to be the same in both bands, the change in the bottom index is

$$\Delta Y_i = \frac{K_j - K_i}{\sqrt{(K_i^2 - K_j^2)}} \frac{\Delta r}{r} \tag{7}$$

Thus, the sensitivity to changes in bottom reflectance is largest for bands having the greatest difference in attenuation coefficients. On the other hand, this difference cannot be indefinitely increased without simultaneously decreasing the depth of penetration (approximately $1/K_i$, if K_i is the larger of the attenuation coefficients). Obviously one band should be chosen to minimize K_i, but the other band must be chosen to achieve a compromise between sensitivity and penetration depth. In the data set under consideration, data quality is also a consideration, since the gain settings of some bands were either higher or lower than optimal. For this reason, band C7 was chosen instead of C8 or C9 on the basis of data quality, although these bands had a slightly smaller attenuation, and band C5 was chosen to balance sensitivity against penetration depth.

Having selected the wavelength bands and determined the ratio of water attenuation coefficients for these bands ($K_7/K_5 = 0{\cdot}52$), the bottom-type index was calculated point-by-point for the scene, and an output image was generated from this index. This image is shown in figure 2, along with the single-band images for bands C7 and C5. Exposed land areas were edited out using the thermal band, and appear as white in these images. The image brightness in figure 2 (*c*) may be interpreted as being approximately proportional to the bottom reflectance (neglecting spectral variations in the reflectance), whereas figures 2 (*a*) and (*b*) are influenced by water depth as well as bottom reflectance. Thus, the darker areas on the left-hand side of the single-band images appear as a brighter tone on the bottom image, since these areas are characterized by a large water depth but a fairly highly reflecting bottom. The dark areas near

...on the other hand, appear dark on all the images since they correspond to ...ed areas in shallow water. A further evaluation of these results is presented in

5. Landsat data analysis

Analysis of the Landsat data set for frame 2993-14385 proceeded in a similar manner to the aircraft data set. Deep water signals were calculated for an area off the edge of the Bank west of North Cat Cay, and scatter plots of X_1 (MSS 4) versus X_2 (MSS 5) were generated for several areas. Owing to the coarser spatial resolution, areas of uniform bottom type are somewhat more difficult to find, and the set of usable data points is smaller. Figure 3 shows a scatter plot for an area south of North Cat Cay which appears to be relatively homogeneous. The ratio of attenuation coefficients obtained from this set of points is 0·24.

Using the deep-water signals and the ratio of attenuation coefficients determined from the above analysis, the bottom-type index (Y_1) was generated point-by-point for the portion of the frame covering the North Cat Cay test site. The image generated from this index is shown in figure 4, along with the raw data images for MSS 4 and MSS 5. Land was edited out from these images using the signal in MSS 7 (0·8–1·1 μm) to discriminate between land and water. A small geometric correction was also applied to this data to correct for image skew due to earth rotation effects.

Making allowances for the difference in spatial resolution, the Landsat bottom map (figure 4 (c)) is similar to the aircraft bottom map (figure 2 (c)) in the shallow-water areas near the islands. In deeper water, on the left-hand side of the scene, the Landsat image is generally noisier and has a higher proportion of dark bottom classifications. This is probably due to the relatively higher water attenuation in MSS 5 than in band C5 of the aircraft scanner, and the lower signal-to-noise ratio of the Landsat scanner. There is also a dark spot in the Landsat image south of North Cat Cay, which is caused by the shadow of a small cloud appearing in the lower right corner of the image.

6. Evaluation of results

The results of the bottom reflectance mapping algorithm were evaluated by direct observations of the bottom conditions at nine stations within the test site. The

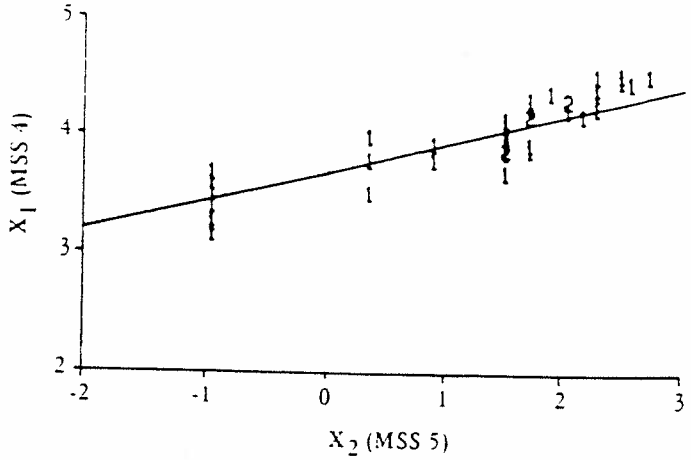

Figure 3. Scatter plot of X-values for Landsat bands MSS 4 and MSS 5 over sand bottom near North Cat Cay. Line indicates least-squares fit to data.

locations of the stations are shown in figure 5, and a summary of the observations is contained in table 3. The bottom reflectances indicated in table 3 were obtained by analysing underwater photographs of the bottom, examples of which are shown in figure 6. Each photograph included a calibrated grey scale having reflectances of 1·8, 8·6 and 28·7 per cent for each panel. The photographs were scanned with a microdensitometer to determine the film density for each grey panel and for the bottom. The grey panel readings were used to obtain a relationship between film density and panel reflectance, which was then used to infer the bottom reflectance. Adequate sampling of the bottom reflectance is a problem, since the field of view of the underwater camera is much smaller than the resolution of the remote sensing data. In order

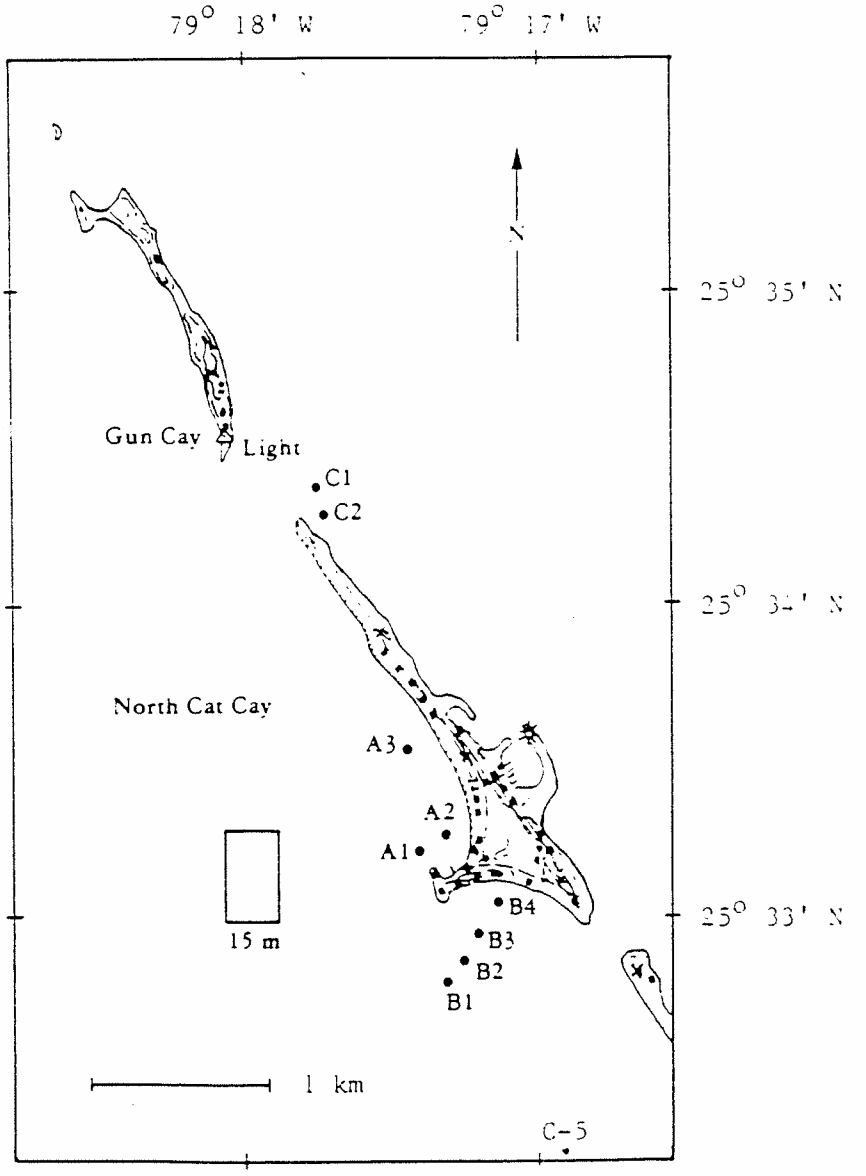

Figure 5. Map of test site showing locations of measurement stations and 15 m test location.

Table 3. Summary of bottom observations at test locations.

Station	Depth (m)	Reflectance (per cent)	Description
A1	3	16·0	Boundary of vegetated areas
A2	3	5·0	*Thalassia* bed
A3	3	32·0	White carbonate sand
B1	5	16·5	Hard, non-vegetated bottom
B2	4	30·0	White carbonate sand
B3	3	12·5	Boundary of vegetated area
B4	4	5·0	*Thalassia* bed
C1	3	35·0	White carbonate sand
C2	4	3·0	*Thalassia* bed

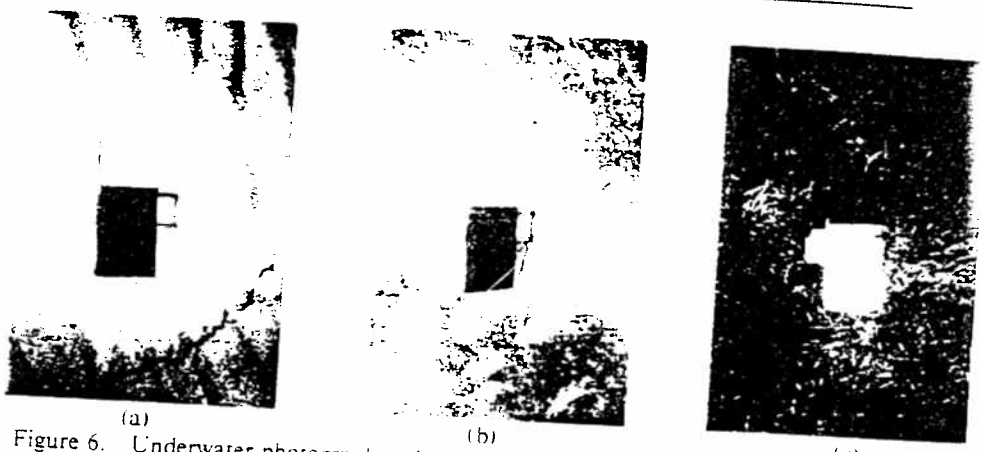

Figure 6. Underwater photographs taken near North Cat Cay: (*a*) Station B1 (hard, non-vegetated bottom); (*b*) Station B2 (white carbonate sand); (*c*) Station C2 (*Thalassia* bed).

to alleviate this problem, attempts were made to locate the stations in relatively homogeneous areas, with the exception of stations A1 and B3 which were located at the boundaries of vegetated areas.

After processing the aircraft and Landsat data, the coordinates of each station were determined by overlaying a map (figure 5) on the processed image. The bottom-type indices (the Y-values) were then extracted from the digital data at each station. These values are plotted versus the measured bottom reflectances in figure 7. The Y-values are proportional to the log of the bottom reflectance as predicted by equation (3). For the aircraft data, the Y-value predicts the bottom reflectance with a standard error of 1·8 reflectance units. For the Landsat data the standard error is 3·6 reflectance units for the nine measurements. It may be noted that over the range of depths for which bottom reflectance measurements were made, the single-band radiances are fairly good predictors of the bottom reflectance. This is not expected to be true over a wider range of depths, however, since water attenuation effects would cause a larger variance than bottom reflectance changes. To test this expectation, an area further offshore was selected (see box in figure 5) which has a depth of approximately 15 m and a bottom composed of white coral and sand, according to DMA chart No. 26324. Colour aerial photography seems to indicate a bottom similar to that at station B1, although the difference in depth makes the bottom type somewhat difficult to judge. Single-band data values and Y-values were extracted from both the aircraft and

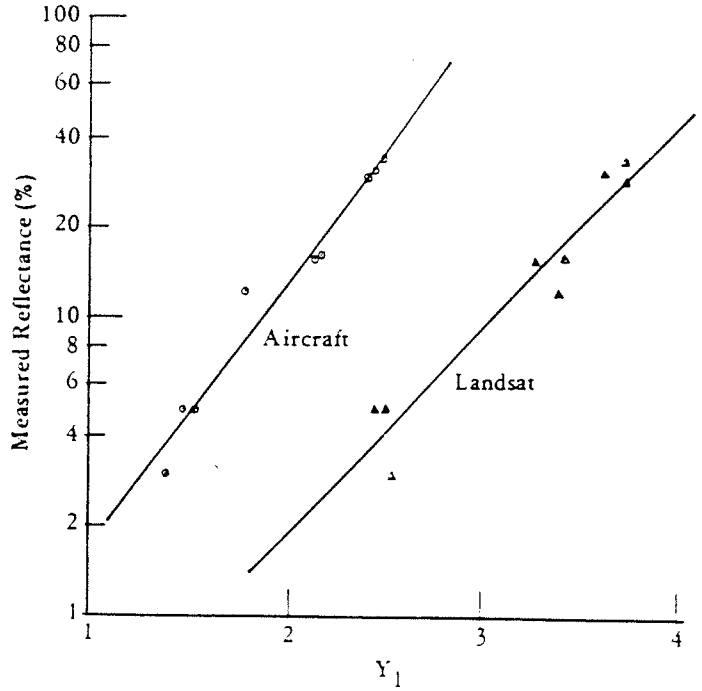

Figure 7. Bottom-type indices calculated from aircraft and Landsat data versus measured bottom reflectances at nine stations. Lines indicate least-squares fit to data points.

Landsat data sets for this area and used to calculate the bottom reflectance. Using a regression fit between the single-band data values and the bottom reflectances at the nine stations, the bottom reflectances predicted by C5 and C7 are 2·8 and 6·7 per cent respectively, both of which are much too low. The bottom reflectance predicted by the *Y*-value for the aircraft data is 21·8 per cent, which is probably quite close to the correct value judging from the reflectance at B1. For the Landsat data the MSS 5 radiance is not significantly above the deep-water radiance, so the bottom reflectance cannot be reliably calculated : if this calculation is attempted, one obtains a reflectance of 7·4 per cent, which is in fact much too low.

The results of the water optical parameter determination may be evaluated by a comparison with field measurements of the irradiance attenuation coefficient. Unfortunately, no exactly simultaneous field data are available. However, as mentioned earlier, two measurements were made near the test site within a week of the Landsat overpass, which indicate at least the range of attenuation coefficients occurring there. The first measurement was made on 4 October 1977 just south of North Cat Cay (Station C-5, 25° 32·2′N, 79° 16·9′W) while the second measurement was made on the following day west of Bimini (Station D-7, 25° 43·9′N, 79° 18·2′W). The attenuation coefficients measured at station C-5 were 0·080 m^{-1} for MSS 4 and 0·352 m^{-1} for MSS 5. The corresponding values measured at D-7 were 0·134 m^{-1} and 0·408 m^{-1} respectively. The higher attenuation at D-7 is thought to be due to resuspension of sediments during high wind conditions occurring on 4 and 5 October. Winds were calm prior to the Landsat overpass and the attenuation coefficients probably returned to the values measured at C-5. The ratio of attenuation coefficients extracted from the

Landsat data was 0·24, which is within 10 per cent of the measured value at C-5. The ratio of attenuation coefficients obtained from the aircraft data for a similar pair of wavelength bands (C7 and C4) was 0·33, which is closer to the value measured at Station D-7. Since the aircraft data was collected some 10 months later, not too much significance can be placed on this comparison, but the attenuation parameters obtained from the aircraft data analysis are apparently within reasonable limits.

7. Conclusions

Multispectral scanner data collected from aircraft or satellite platforms can be used to infer relative water attenuation coefficients in shallow water, provided that the water is well mixed and a relatively homogeneous bottom exists over a range of water depths. The scanner data can also be used, in conjunction with the processing algorithm described in this paper, to map bottom reflectance variations without knowledge of the water depth. The performance of this algorithm depends upon the system characteristics and the wavelength bands used, but can give apparently accurate results to a depth of 15 m in clear ocean water with the proper choice of wavelength bands. Landsat is not optimally suited in this regard, since only one of its bands can penetrate to depths larger than about 5 m. However, within this range fairly accurate results can also be obtained from Landsat data.

Acknowledgments

The author wishes to thank Mr. Robert Shuchman for his assistance in taking the underwater photographs, and Mr. James Hillier for providing logistical support for the field measurements.

The analysis phase of this research was supported by the Office of Naval Research, Contract N00014–78–C–00458. Portions of the data collection were supported by the Defense Mapping Agency, contract DMA800–77–C–0053.

References

HASELL, P., PETERSON, L., THOMSON, F., WORK, E., and KRIEGLER, F., 1977, Active and passive multispectral scanner for earth resources applications: an advanced applications flight experiment, Report No. 115800–49–F, Environmental Research Institute of Michigan, Ann Arbor, Michigan.

JERLOV, N. G., 1976, *Marine Optics* (New York: Elsevier).

LYZENGA, D., 1978, *Appl. Optics*, 17, 379.